Shear-induced effects in hyperbranched-linear polyelectrolyte complexes

G. K. Dalakoglou,[1] K. Karatasos,[1,a)] S. V. Lyulin,[2] and A. V. Lyulin[3]
[1]*Physical Chemistry Laboratory, Chemical Engineering Department, Aristotle University of Thessaloniki, 54124 Thessaloniki, Greece*
[2]*Institute of Macromolecular Compounds, Russian Academy of Sciences, Bolshoi Pr. 31, 199004 St. Petersburg, Russia*
[3]*Group Polymer Physics, Eindhoven Polymer Laboratories, Technische Universiteit Eindhoven, P.O. Box 513, 5600 MB Eindhoven, The Netherlands and Dutch Polymer Institute, P.O. Box 902, 5600 AX Eindhoven, The Netherlands*

(Received 4 March 2008; accepted 5 June 2008; published online 15 July 2008)

Static and dynamic properties of complexes formed by hyperbranched polymers with linear polyelectrolytes are studied under the influence of steady shear flow by means of Brownian dynamics simulations. Models of peripherally charged hyperbranched molecules bearing two extreme topological structures and different molecular weights complexed with linear neutralizing chains are subjected to a range of shear rates starting from a low-shear regime toward the complex-breaking point. Examination of the stability limit, shape and mass distribution parameters, and dynamics in different lengths and timescales is performed as a function of the applied shear. The results described illustrate features of the generic behavior that should be expected from such systems under conditions of steady shear flow. © *2008 American Institute of Physics*.
[DOI: 10.1063/1.2952518]

I. INTRODUCTION

Noncovalent complexes of polyelectrolytes with oppositely charged macroions are commonly used to model the behavior of biological analogs such as protein-DNA systems.[1,2] More recently, systems formed by an association of hyperbranched polymers (HPs) with polyelectrolytes of synthetic or biological nature have been recognized as promising systems for a broad range of novel nanoscale applications.[3–6] Attributes of HPs such as their elevated surface/mass ratio which enhances functionality[7] without practically affecting desired transport properties,[8] combined with the versatility of a detailed manipulation of their chemical characteristics[9] which can allow control of their response to thermodynamic and/or other external stimuli, render them ideal candidates when nanosized multifunctional complexes are required.[10]

In several of these uses an optimal performance of such systems is based on their ability to remain intact under conditions of high hydrodynamic stress, while preserving the intended functionality. For instance, complexes of HPs with proteins or DNA for gene transfection applications[11–15] should maintain their structural integrity and be effectively transported to the target site, while preserving those attributes (such as effective charge, size, and shape) necessary for the final success of the process. If such systems are, e.g., intravenously administered, they can be subjected to shear stresses of the order of 10^3–10^4 s^{-1} in blood flow,[16] which may induce severe shape deformation and/or disruption of the complexes, rendering them inappropriate for the desired usage.[17,18]

The response of HPs under an applied strain as well as several key properties of their complexes with other charged moieties has been found to depend on molecular weight (size) and on a number of structural characteristics such as shape, branch flexibility, and local density.

Because of their distinct structural features, the HPs exhibit a different rheological behavior compared to linear polymers (LPs), either in bulk[19–23] or in solutions and in mixtures with nonhyperbranched molecules.[24–29] The transition from the Newtonian to the shear-thinning regime occurs at higher shear rates, while in the Newtonian regime they exhibit a lower viscosity compared to LP systems of comparable molecular weight.[30–32] These observations have been attributed to their highly branched structure which drastically affects their deformability and their final shape under shear flow.[20,26,33] Moreover, subtle differences in their rheological properties can be observed depending on the details of their branching topology.[29]

In the same context, a direct link between the geometrical characteristics of these systems and the manifestation of changes in the intrinsic and shear viscosity has been established; it was found that the onset of the shear-thinning regime practically coincides with a prominent change in their geometrical features, suggesting that the analysis of shape parameters could be used as an indicator of expected changes in the rheological properties and vice versa.[26,33]

The mechanisms involved in the manifestation of static and dynamic properties in noncovalent complexes between hyperbranched molecules and linear polyelectrolytes in equilibrium have been investigated in detail by means of computer simulations.[34–37] In neutral complexes (i.e., where the total charge of the LP equals in magnitude to that of the HP molecule) comprised by HPs bearing a perfect or almost-

a)Author to whom correspondence should be addressed. Electronic mail: karatas@eng.auth.gr.

perfect dendritic structure, it was found that both static and dynamic properties of the HP constituents were very close to those of the noncharged analogs. Differences, however, have been detected when the HP constituent was characterized by a more "open" structure bearing the dendritic branching units close to the periphery.[34,38] For all complexes, however, it was found that either in terms of conformational characteristics or in terms of global dynamics, the behavior of the linear chains was altered compared to their neutral counterparts, particularly when the size of the HP molecule was increased.

In this work we report on static, dynamic, and conformational characteristics under steady shear of a series of complexes comprised by terminally charged nonregularly branched HPs and neutralizing linear chains. The HP constituents bear different sizes and extremely different branching structures allowing the assessment of the effects of molecular weight and topology on their response under shear flow. As it was demonstrated in our previous work where their equilibrium properties were examined,[34,38] complexes formed by HPs that are characterized by a dense branching pattern throughout the structure exhibit properties similar to those of systems formed by perfect dendritic analogs; this similarity allows them to be considered as cost-effective alternatives in relevant applications. On the other hand, complexes formed by the more open-in-structure, peripherally branched HPs exhibited remarkable differences from the former, both in static and in dynamic properties.

Utilizing as a reference point the information acquired by the investigation of the equilibrium properties, we intend to explore in the present study the range of structural integrity of the complexes, as well as the effects in local and global conformational features upon application of hydrodynamic deformation, as a function of size, HP topology, and magnitude of the applied strain. To assess possible effects from complexation, we have also studied under the same conditions the behavior of the noncomplexed neutral analogs (referred to as *single*) of the HPs that appear in the complexes.

II. MODEL DESCRIPTION AND SIMULATION DETAILS

Brownian dynamics simulations in the presence of shear flow have been performed following the Ermak–McCammon algorithm[39] as in authors' previous works.[26,36] Brownian dynamics stochastic differential equation is integrated forward in time[39] according to

$$\vec{r}_i = \vec{r}_i^0 + \frac{\Delta t}{k_B T}\sum_j \mathbf{D}_{\mathbf{ij}}^{\mathbf{0}} \cdot \vec{F}_j^0 + \vec{v}_i^0 \cdot \Delta t + \vec{\Phi}_i^0(\Delta t), \tag{1}$$

where $\vec{r}_i^0$ is the position vector for bead i before the Brownian dynamics time step Δt, $k_B T$ is the Boltzmann factor, $\mathbf{D}_{\mathbf{ij}}^{\mathbf{0}}$ is the diffusion hydrodynamic tensor, and $\vec{v}_i^0$ is the velocity of the solvent at the position of bead i, where for steady shear flow $v_{i,x}^0 = y_i^0 \dot{\gamma}$, with $\dot{\gamma}$ representing the shear rate. The solvent is considered to be a structureless continuous medium in which the bead-solvent collisions are mimicked through a random force $\vec{\Phi}_i^0$. Hydrodynamic interactions are taken into account explicitly through the Rotne–Prager–Yamakawa tensor.[40,41] The strength of the hydrodynamic interactions is regulated by the dimensionless parameter $h^* = (3/\pi)^{1/2} a/l = (3/\pi)^{1/2} \zeta/(6\pi\eta_s l)$, where η_s represents the solvent viscosity and a is the Stokes hydrodynamic radius of a single bead. ζ denotes the single bead friction coefficient. To allow comparison to the results from previous studies[26] h^* is taken to be equal to 0.25.

The principal physicochemical interactions of beads are taken into account rigorously by means of appropriate potentials, giving a total force $\vec{F}_j^0$[Eq. (2)],

$$\vec{F}_j^0 = \sum_k \mu_k \left(\frac{\partial \nu_k}{\partial \vec{r}_j}\right)_r^0 - \frac{\partial U_{LJ}}{\partial \vec{r}_j^0} - \frac{\partial U_C}{\partial \vec{r}_j^0}. \tag{2}$$

In Eq. (2) ν_k is the equation of rigid constraint for the kth bond, μ_k is the corresponding Lagrange multiplier, U_{LJ} corresponds to Lennard-Jones potential for excluded-volume interactions, and U_c to Debye–Hückel potential for electrostatic interactions.

All the nonbonded beads in a complex interact via a Lennard-Jones potential,

$$U_{\mathrm{LJ}}(r_{ij}) = 4\varepsilon_{LJ}\left[\left(\frac{\sigma}{r_{ij}}\right)^{12} - \left(\frac{\sigma}{r_{ij}}\right)^{6}\right], \tag{3}$$

where r_{ij} is the distance between ith and jth beads, $\varepsilon_{\mathrm{LJ}} = 0.3 k_B T$ and $\sigma = 0.8l$ as in our previous work[34] are the characteristic energy and length parameters, and r_{cut} is the cutoff distance ($r_{\mathrm{cut}} = 2.5\sigma$). The attractive interactions between charged beads in Eq. (3) are omitted.

Coulomb interactions of charged beads are taken into account through the Debye–Hückel potential,

$$\frac{U_C}{k_B T} = \lambda_B |q|^2 \sum_{i,j} \frac{\exp(-r_{ij}/r_D)}{r_{ij}}, \tag{4}$$

where r_{ij} is the distance between ith and jth charged beads with charge equal to q(herein $|q| = 1$), λ_{B} is the Bjerrum length describing the strength of Coulomb interactions in a dielectric medium and r_D is the Debye length which describes the screening of the electrostatic interactions due to the presence of counterions and salt in real solutions. Since the main effect of electrostatic interactions is expected when the Debye length exceeds the complexes' size, we have adopted a sufficiently large value of $r_D = k^{-1} = 8.96l$ which corresponds to low aqueous salt concentration,[17] as was used in past studies in charged dendrimer systems[42] and in complexes with linear polyelectrolytes.[34,36] For complexes like the ones studied in this work, where the HP charge is fully compensated by the charge of the linear chain, counterion condensation is expected to be only of minor importance, and therefore the presence of counterions is not taken into account.

The SHAKE algorithm with relative tolerance of 2×10^{-6} is used to maintain a fixed bond length.[43] Dimensionless quantities used in the simulations such as bond length l, thermal energy $k_B T$, translational friction coefficient ζ, and time $\tau = \zeta l^2/k_B T$ are set to unity, while dimensionless integration step chosen as $\Delta t = 10^{-4}$. Dimensionless shear rate is set as $\dot{\gamma}^* = \dot{\gamma}\zeta l^2/k_B T$.

Polymer constituents of the simulated complexes are represented by freely jointed bead-rod structures. Hyper-

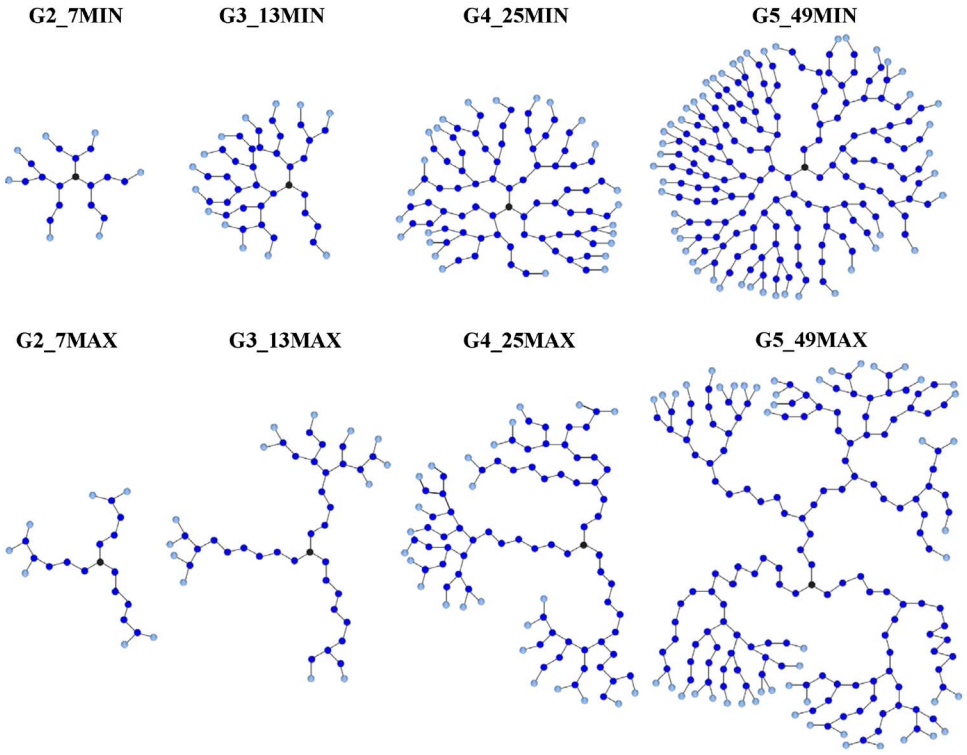

FIG. 1. (Color online) Schematic representations of two dimensional projections of the studied HP models participating in the complexes examined. Charged (terminal) beads are shown in different colors.

branched structures are characterized according to their number of monomers, N and degree of branching (DB), which is defined as $DB=2D/(2D+L)$, where D is the number of fully branched monomers and L the number of linear beads, respectively.[34,44] Apart from DB, Wiener index (WI) is also used in order to describe topologically the different structures.[45,46] WI is the cumulative distance between all pairs of beads measured in terms of the number of intervening bonds between them. Herein it is calculated according to the expression[47] $WI=\Sigma_{s=1}^{N-1}(V_{L,s}\times V_{R,s})$, where $V_{L,s}$ and $V_{R,s}$ are the numbers of beads in the left and in the right, respectively, of the center of each bond s. Therefore, N, DB, and WI uniquely define the structure of the systems studied.[29,47]

HPs with total number of beads corresponding to generations 2, 3, 4, or 5 of perfect dendrimers were utilized. DB of all the HP structures is chosen to be equal to 0.5 which stands between perfect dendrimer and linear chain.[44,48] The number of terminal beads of each HP structure depends solely on its DB.[45] For each of the above mentioned HP structures bearing a lower value of WI (min), which corresponds to a rather compact interior, as well as structures of higher WI (max) closer to a more open starlike shape, were examined. Each one of the HP terminal beads was set to carry a positive unit charge. Linear chains were selected to have a total number of beads equal to the number of terminal beads of the corresponding HP. Each linear chain bead was set to carry a negative unit charge, preserving thus the overall electrostatic neutrality of the system.

In total, eight model complexes were constructed and simulated, as depicted in Fig. 1. Details of their characteristics are listed in Table I.

The initial configurations were equilibrated for about 10^7 time steps each, depending on their size, and then production runs typically of 1.4×10^7 steps were performed applying a predetermined value of shear rate.

III. CRITICAL SHEAR RATE

Following the above described procedure, runs of systematically increased shear rates were conducted, until at a

TABLE I. Structural details of the simulated systems.

		HP (DB=0.5)					LP	Complex
	Systems	WI	N	Equivalent generations	Pseudo-generations	N_T	N_L	N_{tot}
1.	G2_7MIN	990	22	2	3	7	7	29
2.	G2_7MAX	1327			5			
3.	G3_13MIN	6384	46	3	5	13	13	59
4.	G3_13MAX	9710			8			
5.	G4_25MIN	37670	94	4	6	25	25	119
6.	G4_25MAX	60351			11			
7.	G5_49MIN	210 726	190	5	8	49	49	239
8.	G5_49MAX	333 493			15			

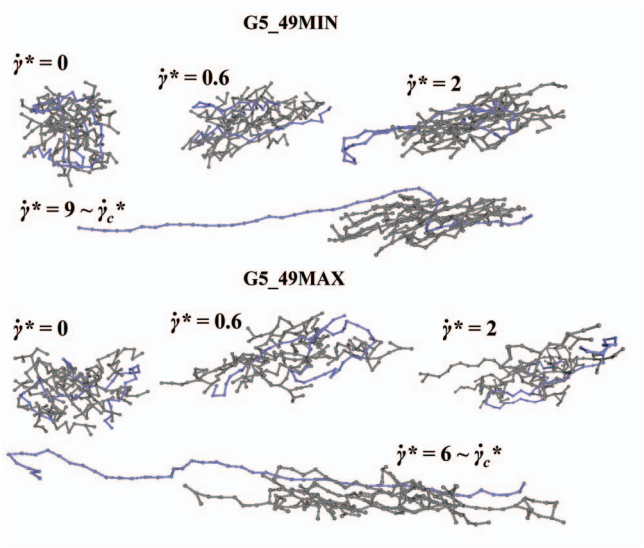

FIG. 2. (Color) Snapshots of the G5 complexes both of minimum and maximum WI architectures.

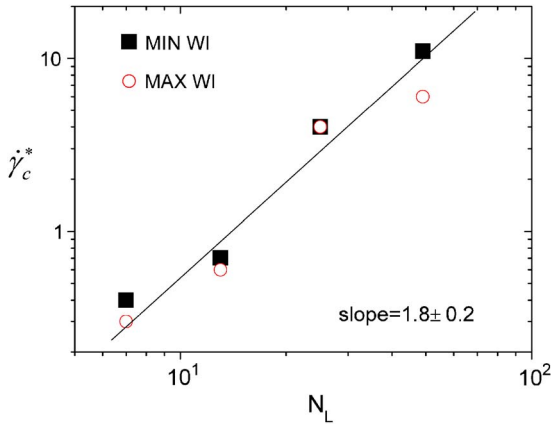

FIG. 4. (Color online) Dependence of the critical shear rate on the molecular weight of the LP. The solid line denotes the slope which describes the data.

characteristic shear rate $\dot{\gamma}_c^*$, the two complex constituents started to separate, leading gradually to decomplexation between the HP and LP molecules. This critical value of shear rate signified the point at which shear forces overcame on average the attractive electrostatic forces between the charged beads of the two constituents. Figure 2 shows snapshots of two of the examined systems, representing conformations at different shear rates up to the onset of decomplexation.

The definition of $\dot{\gamma}_c^*$ follows a criterion, which is based on the distance between the centers of mass of the hyperbranched and the LP that form the complex. The value of shear rate, at which this distance assumes a value much higher than the size of the complex, is taken as the critical value, provided that no such instance was observed in the full-length runs at all lower shears examined for each model. Following this procedure, the value of $\dot{\gamma}_c^*$ was determined by performing runs differing by steps of $\delta\dot{\gamma}^*=0.1$ or $\delta\dot{\gamma}^*=1$ depending on the size of the model. These instances of complex dissociation in runs at $\dot{\gamma}_c^*$ that is taken to be the critical value are shown in Fig. 3.

Figure 4 depicts the dependence of $\dot{\gamma}_c^*$ on the molecular weight of the LP. Apparently, $\dot{\gamma}_c^*$ exhibits a systematic variation with the molecular weight of the linear chain (i.e., on the number of the charged beads), which appears to be independent of the HP topology. The critical shear rate values of models bearing the same molecular weight are (within the

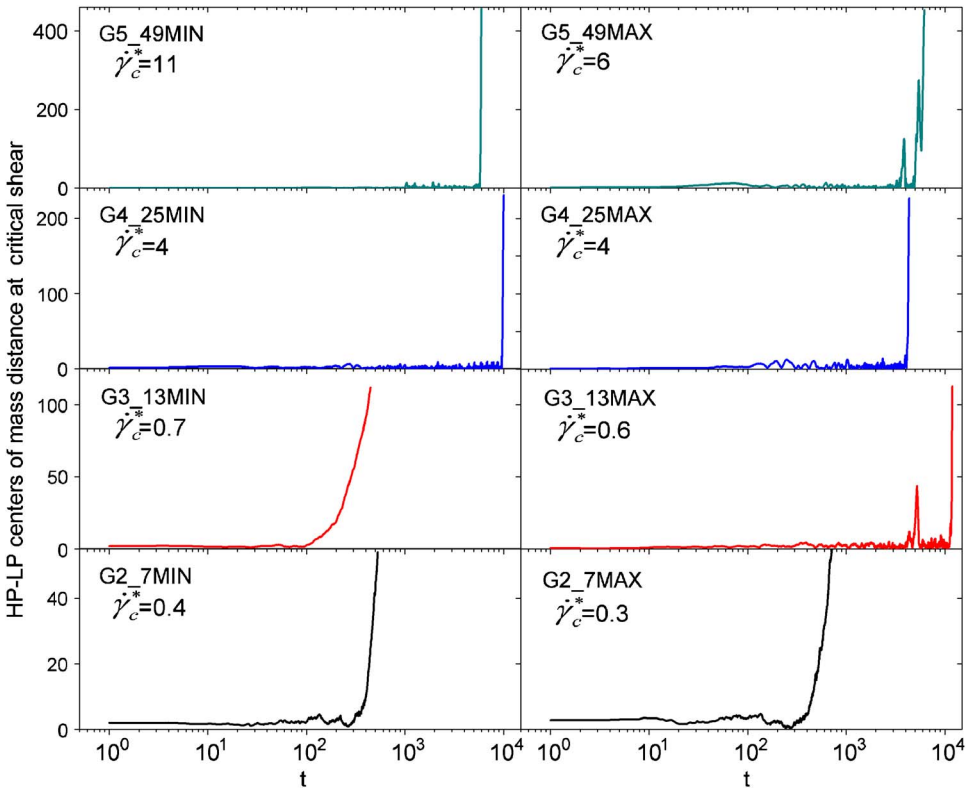

FIG. 3. (Color online) The instances of dissociation between the HP and LP components of the examined complexes.

accuracy of determination) the same. Only at the larger examined models the difference between the values of critical shear rate corresponding to the minimum and the maximum WI models seems to exceed this margin. This occurrence might be related to the larger degree of deformability of the more open in structure maximum WI models (particularly the larger in size, see Fig. 1) compared to their minimum WI analogs as will be shown later (Sec. IV, Fig. 6), which results to the onset of deformation at lower shear rates and thus to an earlier (in terms of the applied shear stress) decomplexation of the corresponding complexes. Overall, the observed behavior can be well described by a power law $\dot{\gamma}_c^* \propto N_L^a$, where $\alpha = 1.8 \pm 0.2$ provides a good fit for both the examined topologies.

Rationalization of this dependence is in order, if we consider that the critical shear rate is naturally related to the strength of the forces which hold the two components of the complex together. These forces are mainly of electrostatic nature, and their magnitude is proportional to N^2, where N represents the number of the charged beads. Since shear forces are proportional to the applied shear rate, it follows that close to decomplexation, these forces should counterbalance each other rendering for the critical value of shear $\dot{\gamma}_c^* \propto N^2$, or since the number of charged beads of each component is equal to N_L, $\dot{\gamma}_c^* \propto N_L^2$. The difference of the observed exponent from 2 should be attributed to the fact that part of the energy associated with shear force is channeled to the deformation of the complexes.

IV. EFFECTS OF SHEAR ON SIZE AND SHAPE

At quiescent conditions it was found[34] that the molecular weight dependence of the average radius of gyration for HPs in complexes of both topologies followed to a good approximation the $R_g \sim N^{1/3}$ law in agreement with past findings pertinent to HP molecules of regular dendritic topology.[49,50] In the present study, at constant shear rate the same scaling was found to provide a good description of the relation between average size and molecular weight of the complexes, throughout the entire range of shear rates examined (for complexed systems below the critical shear rate). The changes in average size of the HP constituents of the complexes induced by the application of shear are shown in Fig. 5.

Comparison between the behavior of complexes and noncomplexed HPs of both architectures shows that complexation does not incur any significant change to the dependence of their average dimensions on shear rate. For the minimum WI models [Fig. 5(a)] the dependence of R_g on shear rate is described well by that reported from past studies of neutral regular dendrimers of similar size either in solution[27] or in the bulk.[51] For maximum WI models [Fig. 5(b)] the behavior reported for perfect dendrimers [lines in Fig. 5(b)] seems to capture the dependence of the size of these systems on shear rate as well, although a deviation from this dependence in large size models and at high shear rates seems to be developing. The degree of deviation, however, does not lie outside the calculated error margins.

In terms of absolute values of the average size, minimum

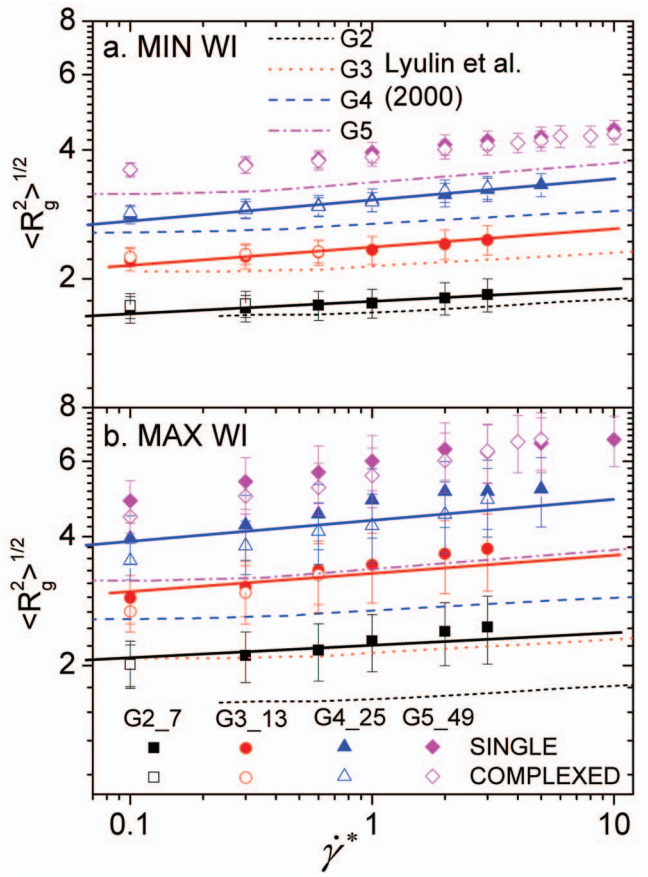

FIG. 5. (Color) Average radius of gyration as a function of shear for all the examined HPs participating in complexes. (a) Minimum WI models and (b) maximum WI models. For complexed HPs, only values of shear below $\dot{\gamma}_c^*$ are considered. For comparison purposes, the dependence of the noncomplexed analogs is shown as well. Noncontinuous lines represent the behavior of perfect dendrimer analogs from Lyulin *et al.* (Ref. 15), while the solid lines denote the slopes reported in studies of regular dendrimer melts of the corresponding generations from Bosko *et al.* (Ref. 34).

HPs exhibit moderately larger dimensions compared to analogous dendrimer models which ranges from about 8% to 16% as we move from the lower to the higher molecular weights examined. This relative increase in size is rather insensitive to shear rate and can be attributed to the existence of imperfections in the branching pattern of minimum HP models compared to that of regular dendrimers. Comparison of the average size between the minimum and maximum WI systems shows that maximum WI systems assume larger dimensions. The ratio of R_g's between HPs of the two topologies starts from the zero-shear value[34] of about 1.3 for very low shear rates and reaches a value of approximately 1.5 as the molecular weight increases and as we move to the limit of high shear rates. To get a better insight on the relative changes in shape of the complexes' constituents induced by application of shear, we have examined the dimensions of the corresponding ellipsoids of inertia as illustrated in Fig. 6.

For the larger systems (G4, G5) of both topologies a change in slope (Fig. 6, solid lines) of the longer (a) over the shorter (c) semiaxis of the ellipsoid is observed when shear rate exceeds a threshold value of $\dot{\gamma}^*$. This effect is a combined result of a shear-induced elongation of the HP along the direction of shear, together with the reduction of the di-

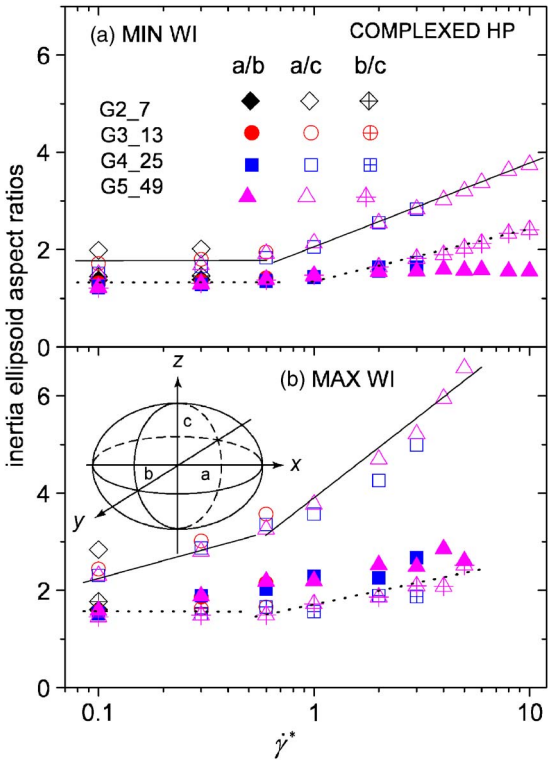

FIG. 6. (Color online) Aspect ratios of the ellipsoid of inertia semiaxes, of the HPs in complexes. (a) Minimum WI models and (b) maximum WI models. Lines are guides to the eye and indicate changes in slopes. The solid lines describe the behavior of the a/c ratio, while the dotted lines follow that of the b/c ratio.

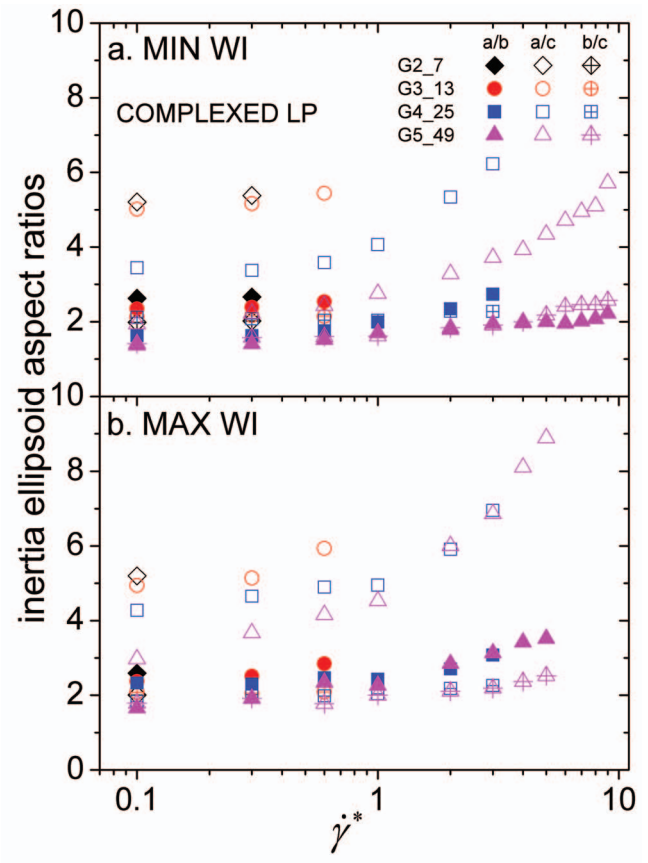

FIG. 7. (Color) Strain rate dependence of the ellipsoid of inertia aspect ratios for the linear chains participating in complexes comprised by (a) minimum WI and (b) maximum WI HPs.

mension of the shorter semiaxis toward an increasingly oblate shape. At a similar shear rate, an analogous change is observed in the b/c ratio (Fig. 6, dotted line), but the effect is less prominent due to the lower degree of deformation along the b semiaxis. A like behavior is also observed in the noncomplexed HP models (not shown here), where the same effect can be observed for the lower molecular weight systems as well. The dependence of shape parameters on shear rate of the LPs participating in complexes is displayed in Fig. 7.

The response of the LPs to strain rate is in close analogy to that characterizing the HPs of the corresponding complexes. The higher degrees of elongation as well as the tendency for a larger lateral broadening in shape observed in the maximum WI HP constituents of the complexes are also reflected to the respective LP behavior. Moreover, an apparent change in slope for LPs in both maximum and minimum WI complexes can also be noted at values of shear rate close to those observed in the respective HP response to shear (Fig. 6). The value of shear rate at which a significant change in shape parameters is observed appears to be only weakly dependent on molecular weight and topology.

V. DEPENDENCE OF BEAD AND DENSITY PROFILES ON STRAIN RATE

To examine the effects of shear on the rearrangement of the beads, we have calculated the corresponding bead number histograms $n(r)$ and the density profiles $\rho(r)$ with respect to the center of mass of the HP component of each complex.

As was described in the zero-shear case,[34] minimum WI systems assume less broad bead number profiles compared to their maximum WI analogs, while the effect of complexation becomes important only in complexes comprised by high molecular weight maximum WI HPs. Application of shear practically does not change the above qualitative picture as far as it concerns the behavior of complexed versus noncomplexed HPs.

As it is depicted in Fig. 8 (the behavior of the other systems is in complete analogy), no appreciable effect is discerned in the profiles between single (i.e., neutral, noncomplexed) and complexed minimum HPs [Fig. 8(a)] for different shear rates. Comparison between the respective maximum WI systems shows that differences observed in lower strain rates are essentially smeared out as strain increases. This can be rationalized by the fact that at the high shear rate limit the degree of overlap between the HP and the LP beads in the complex decreases rapidly as the center of masses of the two components are dragged apart toward decomplexation.

Application of shear in complexes of both topologies results to the broadening of their profiles, to a lesser degree for minimum HP complexes, and to a larger degree for maximum WI systems. The effect of broadening can be understood in connection with the changes imparted in the shape as discussed earlier, since at more deformed geometries the average distance of beads from the center of mass increases.

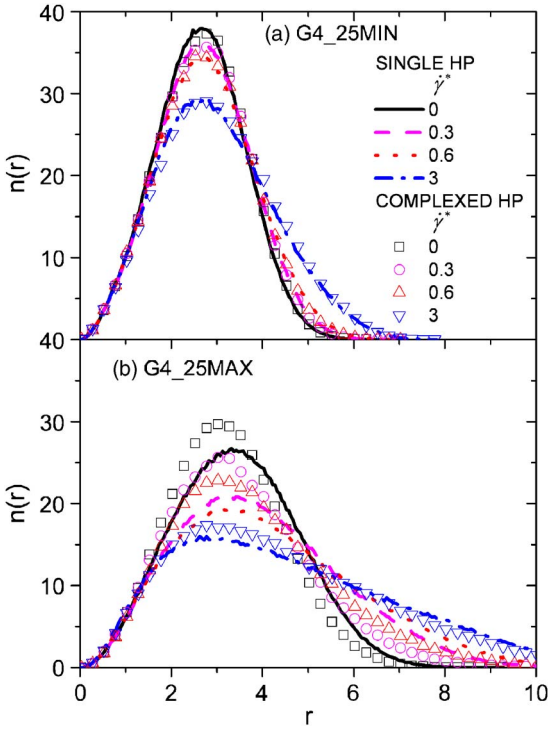

FIG. 8. (Color online) Bead distributions with respect to the centers of mass of the HPs, in complexed (symbols) and in a noncomplexed state (lines) at different shear rates for the G4 systems. (a) Minimum WI and (b) maximum WI.

The differences in profiles between systems of the two topologies (the maximum WI system profiles being broader) should be ascribed to the same origin as in the zero-shear case:[34] The much denser branching pattern of minimum WI HP architectures renders them less deformable compared to their maximum WI HP counterparts where the more open interior allows a larger degree of deformation under the same shear.

The dependence of the corresponding density profiles, calculated from the bead profiles divided by the volume of a spherical shell between distances r and $r+\delta r$ from the HP center of mass, is shown in Fig. 9 for the higher molecular weight systems where a larger range of shear rates prior to decomplexation can be explored.

At distances from the center of mass below one bond length, no systematic trend can be observed in different shear rates, since in such a small volume the enhanced local density fluctuations can smear out any possible effect. The main effect of shear is reflected at distances larger than $r\sim 2$. The distributions drop faster at intermediate distances upon increase of the shear rate, while developing longer tails toward the periphery. This effect is more prominent in the maximum WI systems. The higher deformability in their shape combined with the existence of a larger population of beads (see Fig. 1) close to their periphery compared to the minimum WI models can account for this behavior. This trend becomes less prominent in the lower molecular weight systems. The differences between the profiles of complexed and noncomplexed HPs (less broader in single systems, not shown here) become observable only in large molecular weight systems

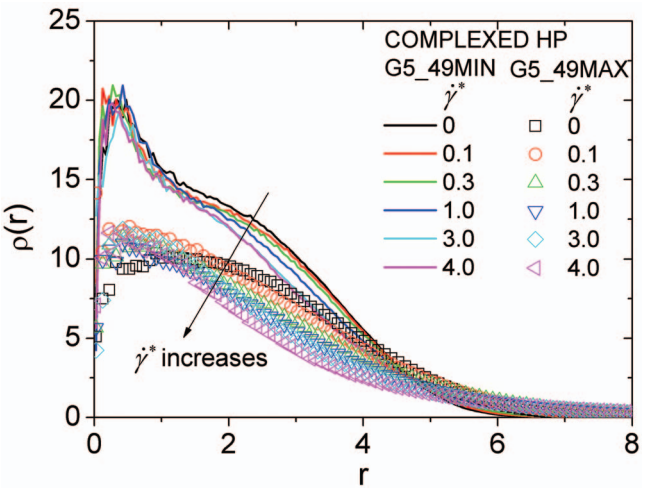

FIG. 9. (Color) Influence of shear rate on the density profiles of HPs participating in complexes of both topologies, for the larger examined systems. The arrow indicates the direction of the increase in shear rate.

(i.e., in G4 and G5 complexes) of the maximum WI topology, in line with the behavior noted in the corresponding bead distributions.

VI. EFFECTS OF SHEAR ON DYNAMIC PROPERTIES

The impact of application of shear on dynamics at local (of the order of a bond) and at global (of the order of the entire complex) lengthscales was examined by monitoring appropriate autocorrelation functions (ACFs). Part of the dynamic spectra obtained were analyzed following the method of the distribution of relaxation times (DRT) (see Ref. 34 and references therein) according to which a correlation function is described as a continuous superposition of single exponential processes: $C(t)=\int_{-\infty}^{\infty}F(\ln(\tau))e^{-t/\tau}d\ln\tau$. Characteristic relaxation times corresponding to different relaxation processes (appearing as different peaks in the distribution) are estimated via the first moment of the calculated distribution function $F(\ln(\tau))$ over the relevant time window. If the entire time window is taken into account, an overall average relaxation time equivalent to integrating the respective ACF is calculated instead. For dynamic processes associated with symmetric peaks in the distribution, the time location of the corresponding peak provides a good estimation of the characteristic relaxation time.

Dynamic spectra of local and global reorientational motions as well as of overall size fluctuations were computed and analyzed for a range of different strain rates.

A. Local reorientational motion

Study of the orientational motion at the lengthscale of a bond was performed by means of the first order Legendre polynomial ACF $P_1(t)=1/N\Sigma_i\langle\vec{u}_i(0)\vec{u}_i(t)\rangle$, where $\vec{u}$ represents a unit vector along a bond and N is the number of bonds considered. Figures 10(a) and 10(b) show $P_1(t)$ spectra for two of the HP models in complexes, corresponding to the third generation (G3) of both the considered topologies and for different shear rates.

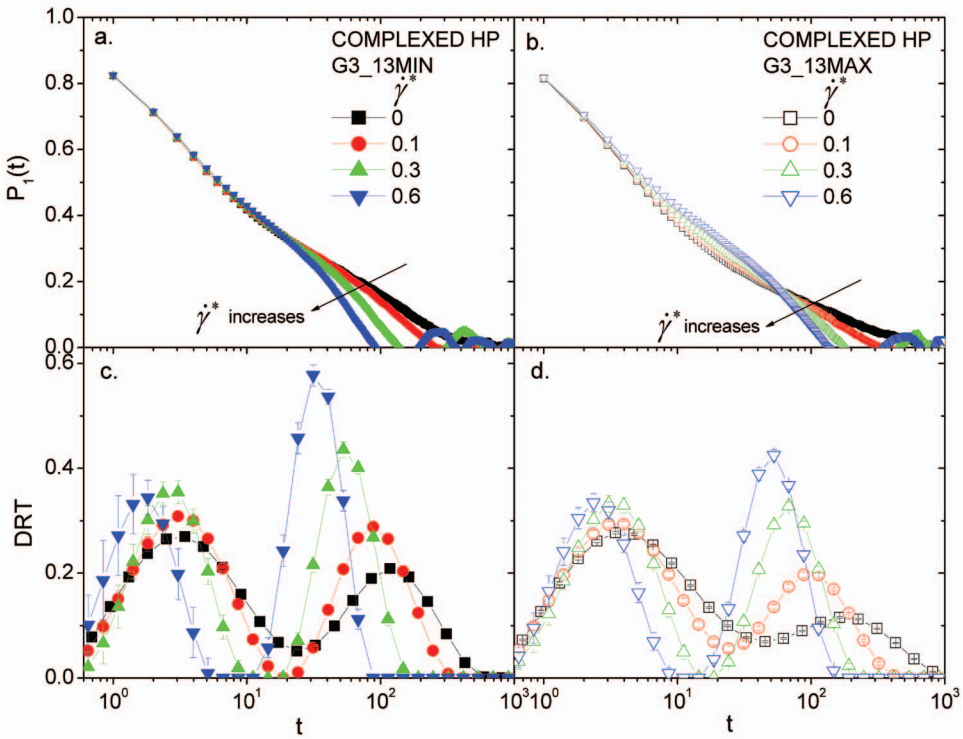

FIG. 10. (Color) Local reorientational spectra of the HP constituents corresponding to different shear rates in complexes of (a) minimum WI and (b) maximum WI topologies. Corresponding DRTs are presented in panels (c) and (d) for complexed HPs bearing the minimum WI and maximum WI structures, respectively.

For comparison purposes, the zero-shear correlation functions are included as well. Figures 10(c) and 10(d) portray the corresponding DRTs. Apparently, the increase of shear rate results to a faster decorrelation (i.e., decay at shorter timescales) of the ACFs for both architectures. Focusing on the features of the respective DRTs, in both architectures and at all shear rates, two processes (peaks) can be distinguished. The origin of these two dynamic processes as was discussed in detail in the zero-shear case[34] (see Fig. 13 in this reference) was the fast, insensitive-in-molecular-weight tumbling motion of bonds, and the slower, molecular-weight-dependent motion of the bonds which requires reorientation of the entire HP molecule for its complete decorrelation (hence the molecular weight dependence). Application of shear clearly shifts the timescale of the slower process (i.e., its peak location) with respect to the zero-shear case toward shorter times even for the lowest applied shear rate. An analogous behavior of the peak representing the faster motion is only observed at shear rates larger than a threshold value (here approximately ~ 0.1). This behavior can be rationalized if we consider that a specific kind of motion will only be affected if the frequency of an external stimuli (here shear) becomes comparable or larger than the characteristic frequency of this motion, i.e., here if $\dot{\gamma}^* \tau \geq 1$, where τ represents the characteristic time of the studied process at rest.[52] For the slower process, this condition holds for all the applied strain rates, while for the faster process only for $\dot{\gamma}^* \approx 0.3$ and larger. The apparent similarity of the distributions describing the fast process [in terms of the location, the width, and the amplitude of the fast peak, Figs. 10(c) and 10(d)] between systems of the two different topologies arises from the local nature of this motion which essentially renders it insensitive to the overall molecular structure.

The behavior of local motion ACFs of noncomplexed analogs as well as that of the LP components as a function of shear rate is qualitatively similar. Therefore no separate discussion will be devoted for their description.

Figure 11 displays the shear rate dependence of the relaxation times corresponding to the observed processes for the maximum WI HP complexed systems. The behavior of their minimum WI counterparts is in complete analogy in terms of the dependence on shear rate. In absolute values, relaxation times corresponding to minimum WI systems are only slightly faster (as also noted for the zero-shear case[34]). Apart from a deviation observed at low shear rates and for low molecular weight samples, both relaxation times exhibit a power law dependence approximately of $\tau \propto \dot{\gamma}^{*-0.7}$.

To illustrate better the effects of shear in local relaxation times as a function of molecular weight, we have plotted in

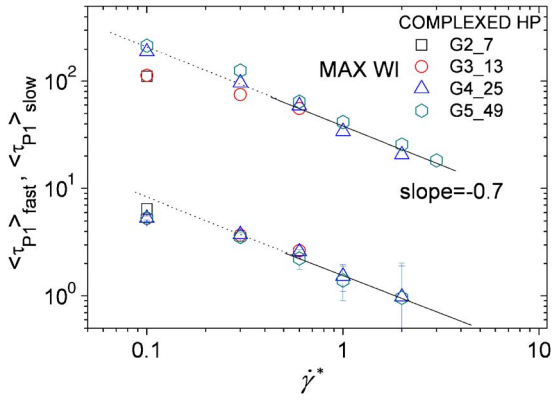

FIG. 11. (Color online) Characteristic relaxation times of the two dynamic processes described in Fig. 10, as calculated through the DRT analysis for the maximum WI systems. Corresponding times for their minimum WI analogs are omitted for clarity. The lines denote the slope which describes the dependence of times of the large size systems at the high-shear limit, for both processes. Error bars are shown if larger than the symbols.

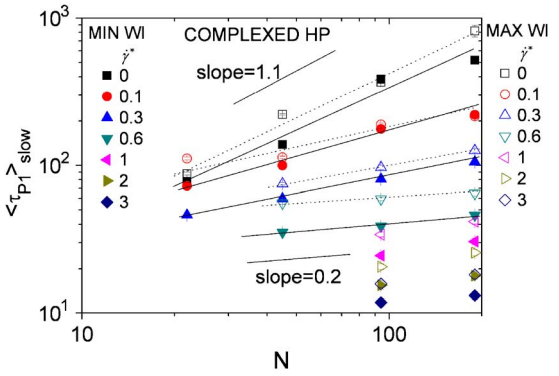

FIG. 12. (Color online) HP molecular weight dependence of the slow process of local reorientational motion in complexed HPs of both the examined topologies for different shear rates. Error bars are comparable to the symbols' size. Lines are guides to the eye for the dependence describing the minimum WI (solid) and the maximum WI (dotted) systems. The values of the slopes at the low and the high shear rates are denoted as well.

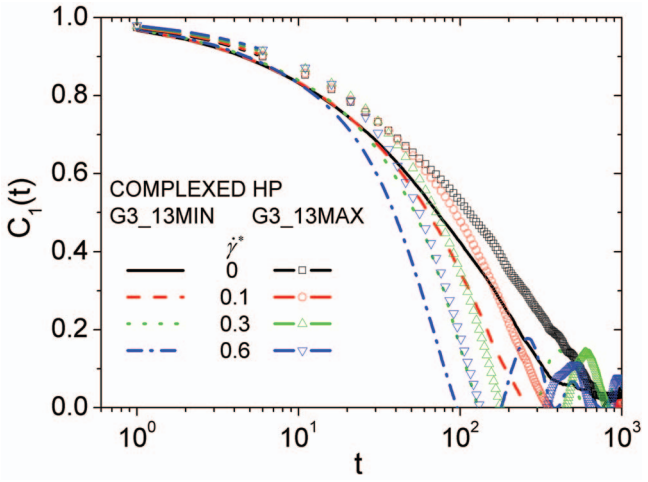

FIG. 13. (Color) Core-to-periphery ACFs for both topologies of the G3 models in complexes at different shear rates.

Fig. 12 the times of the slow process as a function of the number of beads of the corresponding HP components.

Apparently, application of shear imparts a change in slope, which decreases from a slope of ~1.1 corresponding to the zero-shear case to a significantly lower value in the high-shear limit. This behavior appears to be independent of the structural details of the HP molecules. It should therefore be linked to an increasingly significant role of the shape anisotropy rather than the topology and (to a lesser degree) the molecular weight to the average timescale of the overall rotational motion of the complex at high shear rates.

B. Global reorientational motion

As was demonstrated in our past work,[34] the slow mode appearing in local dynamics was directly related to the reorientational motion of the corresponding HPs in the entire molecular scale. To check whether this notion holds true under the influence of shear, we have calculated the ACFs (first order Legendre polynomial) of unit vectors that connect the center of each HP with the beads located at their periphery. These correlation functions can only relax through the global orientational motion of the hyperbranched molecules.[34,49] An example of these ACFs is presented in Fig. 13 for the G3 HP models. A similar qualitative behavior describes the ACFs of HPs in all the examined complexes, as well as of their noncomplexed analogs.

As in the case of ACFs describing local motion (Fig. 10), application of shear accelerates global rotation of the HP molecules (i.e., the relevant correlation functions decay at earlier times). This feature seems to be "inherited" to the behavior of the peak describing the slow process in the local motion spectra [Figs. 10(c) and 10(d)], since the latter is associated with the entire molecule reorientation.

Figure 14 shows the average rotational relaxation times for HPs in complexes of both the examined structures (this picture is representative for the behavior of the noncomplexed HPs as well). The scales in the two axes are different in order to allow a better visual comparison between relaxation times describing the two extreme topologies. The observed dependence on shear rate (at high shear rates) is in line with the one describing the slow process in local motion (Fig. 11).

As follows from the behavior of the high molecular weight systems (for which decomplexation occurs at higher shear rates), a similar slope appears to provide a good description of the global rotational times of the larger models as well. In addition, the molecular weight dependence of this timescale is in complete analogy (in terms of relaxation time values and the respective slopes) to the one illustrated in Fig. 12 for the slow component of the local reorientation, attesting thus to the common origin of these two motional mechanisms.

C. Dynamics probed by the radius of gyration

Dependence of size fluctuations on shear rate for the larger examined models can be examined by means of the ACF of the squared radius of gyration[34] $C_{R_g^2}(t) = \langle R_g^2(0)R_g^2(t)\rangle - \langle R_g^2\rangle^2/\langle R_g^4\rangle - \langle R_g^2\rangle^2$. Such ACFs are presented in Fig. 15 for one of the examined HP complexed systems. The picture describing the behavior of the rest of the examined systems is qualitatively similar. In quantitative terms,

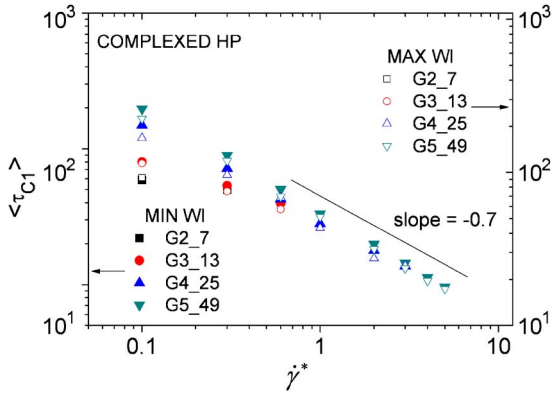

FIG. 14. (Color online) Average global reorientation relaxation times for the HPs participating in complexes as a function of shear rate. Right axis: Minimum WI systems. Left axis: Maximum WI systems. The straight line denotes the slope determined from bond relaxation times (Fig. 11).

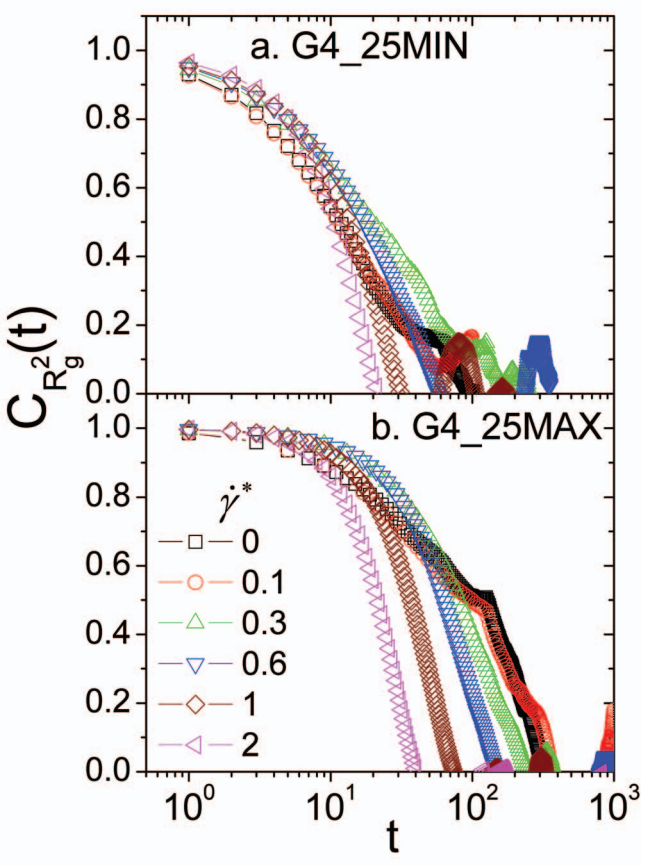

FIG. 15. (Color) Size fluctuation ACFs for the G4 HP models in complexes, at different shear rates for (a) minimum WI and (b) maximum WI topologies.

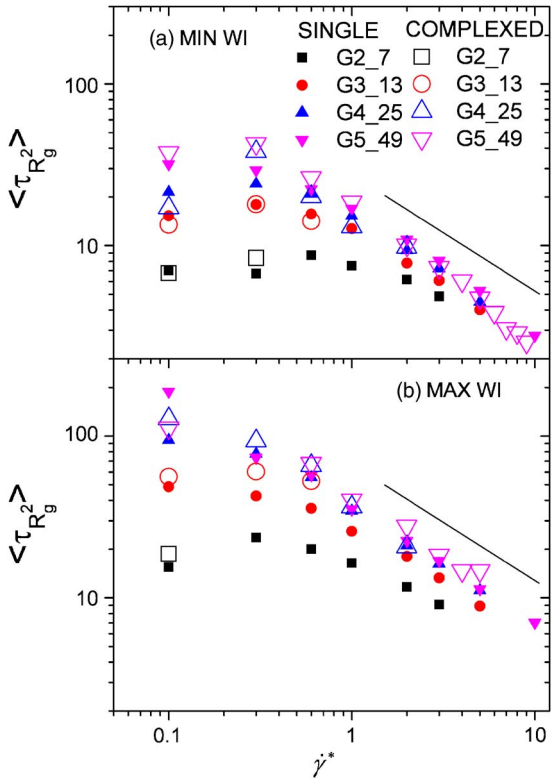

FIG. 16. (Color online) Average relaxation times of $C_{R_g^2}(t)$ ACFs of complexed and noncomplexed HPs participating in (a) minimum WI and (b) maximum WI complexes. The lines denote the −0.7 slope observed in Figs. 11 and 14.

complexed systems appear somewhat slower at low shear rates compared to the respective noncomplexed HP systems.

A notable feature for minimum WI systems is that at shear rates below a characteristic value (here at $\dot{\gamma}^* \sim 1$) the ACFs decay at longer times, while at larger shear rates at a shorter timescale compared to the zero-shear ACF. A similar behavior is observed in the noncomplexed minimum WI HPs as well (not shown here). In the maximum WI complexed HP systems, even a moderate increase in shear rate results to a speedup of the relaxation. However, in noncomplexed maximum WI HPs of the higher molecular weights examined (not shown here), a moderate slow down of the size relaxation was observed at low shear rates. As was also noted in the behavior of the respective systems at zero-shear (see Fig. 17 of Ref. 34), only for the high molecular weight maximum WI systems, a notable difference was observed in the timescale of size fluctuations between complexed and noncomplexed systems. Therefore, particularly in maximum WI systems, the presence of the LP affects appreciably the response of their "breathing motion" to shear.

The corresponding average relaxation times of the $C_{R_g^2}(t)$ ACFs for HPs of minimum and maximum WI topologies, in single and in complexed state, are plotted in Fig. 16. The slope of −0.7 observed in local (Fig. 11) and global (Fig. 14) orientational motion appears to describe well the high shear-limit behavior of the size fluctuations. For the minimum WI systems [Fig. 15(a)], the low-shear behavior is characterized by a weak dependence on shear rate which changes to the high-shear-limit power law beyond a shear value which depends moderately on molecular weight (the smaller the size the higher this threshold value in shear). For the maximum WI systems [Fig. 15(b)], the same picture describes only the lower molecular weight models. The above differences should be ascribed on one hand to the molecular weight dependence of $\tau_{R_g^2}$ at rest (referring to differences observed between low and high molecular size systems at zero shear) and on the other hand to the larger value of the same relaxation time characterizing the maximum WI compared to the minimum WI systems (see Fig. 17 in Ref. 34).

VII. SUMMARY/CONCLUSIONS

In this work we examined the response of static and dynamic properties of complexes formed by terminally charged HPs with linear oppositely charged neutralizing chains, upon application of steady shear. Systems of four different molecular weights and of two distinctly different topologies for each molecular weight were investigated. For comparison purposes, noncomplexed analogs of the HPs participating in the complexes were examined as well.

Study of the stability limits (in terms of structural integrity) of the complexes in the applied shear exhibited a power law dependence on the total molecular weight of the complexes, as well as on the topological WI. Due to the relatively large value of the Bjerrum length considered, the information regarding the dependence of critical shear rate on

size should provide insight in experiments involving electrostatically driven complexes in a low screening environment.

Regarding the effects of shear on average size (Fig. 5), systems comprised by minimum WI HPs practically exhibit the same dependence as that of their regularly branched dendrimer counterparts, possessing though moderately larger dimensions. Maximum WI comprised systems follow a similar dependence of size on shear rate, but in absolute values appear appreciably larger in dimensions compared to the corresponding noncomplexed dendrimer systems due to their more open structure as was also noted in the zero-shear case.[34] Indications for a deviation from the prefect dendrimers' behavior are only noted for larger size systems and at the high-shear limit.

The shape parameters of the examined systems (Fig. 6) show a significant dependence on the applied shear, only after a threshold in shear rate is exceeded. Maximum WI systems show a more sensitive response to shear (i.e., larger relative changes in their geometry) because of the higher deformability allowed by their characteristic branching pattern. The response of the linear chains to shear in terms of their shape anisotropy (Fig. 7), although referring to significantly smaller in molecular weight molecules compared to the respective HP in the complex, follows closely that of the complexed HP, indicating that their conformations are significantly affected by complexation.

Application of shear broadens the bead distributions of the HPs compared to their zero-shear profiles (Fig. 8). This effect is more pronounced in the maximum WI systems. Differences from their noncomplexed counterparts are only observed for the maximum WI systems and only at low shear rates. The density profiles (Fig. 9) of the HPs are dropping faster at intermediate distances from the center of mass for systems of both topologies, while developing tails toward longer distances as an effect of the induced changes in size and shape by the applied shear. Differences in topology are reflected to the larger relative changes with respect to the corresponding zero-shear case, which are observed in the maximum WI systems.

The effects of shear in the dynamic response of complexes (here presented in terms of the HP components) are manifested in motions describing different length- and timescales. In the scale of a bond (Fig. 10), the two processes observed in the absence of shear[34] are also present, and they exhibit a power law dependence of their characteristic time on the applied strain, after the strain rate exceeds their corresponding zero-shear inverse relaxation time. This power law exponent is close to −0.7 for both processes (Fig. 11) and independent of the topology of the examined system. The molecular weight dependence of the slow relaxing process seems to weaken as the shear rate increases (Fig. 12), emphasizing the increasing importance of shape anisotropy rather than the molecular weight at this limit.

This slower mode is also in close agreement in terms of its characteristic time and its dependence on shear, with the timescale describing global reorientation (Figs. 13 and 14). The same power law appears to provide a good description of the high-shear limit of the relaxation time associated with fluctuations in the radii of gyration of the HPs of the complexes (Figs. 15 and 16) of both topologies. In timescales characterizing large lengthscale motions (global reorientation and size fluctuations), differences between systems of distinct sizes and topology are observed mainly in low shear rates (Figs. 14 and 16) and can be considered to have the same origins with those described in the zero-shear state (Ref. 34).

The possibility to follow larger lengthscale dynamic response under shear by monitoring reorientational motion at the segmental level implies that information of large-scale rheological properties can actually be probed by techniques focusing on short time- and lengthscales, such as neutron scattering or NMR.

To summarize the main effects of complexation, topology, and molecular weight under the application of shear, we note that (i) effects of complexation in static properties (bead and density profiles) are mainly manifested in maximum WI HPs only at low shear rates, as well as to the conformational properties of the LPs in complexes (they follow closely that of the HP component) compared to the behavior expected from a noncomplexed linear chain of the same molecular weight. In terms of dynamics, no significant changes are observed in local and global dynamics as a result of complexation. Only the timescale of size fluctuations becomes somewhat slower and only at lower shear rates. (ii) Differences in total molecular weight are significant for the stability limits of the complexes. The larger the complexes, the more stable they are, in the sense that they remain intact at larger shear rates. Higher molecular weight systems assume broader distributions from the smaller systems as expected from their behavior in the zero-shear state,[34] which are amenable to further broadening upon application of shear. In dynamic properties, size influences dynamics only at large lengthscale motions as expected, but the differences observed at low shear rates decrease as the shear rate increases. (iii) The effect of the distinct topology of the two examined categories of HPs is strongly manifested in the sensitivity in deformability of their shape and in the change in mass profiles upon application of shear. Maximum WI systems are more responsive, in the sense that at the same shear rate, they become more anisotropic compared to their minimum WI counterparts, particularly as the shear rate increases. Comparing the dynamic response under shear of systems of the two topologies, it is found that only large lengthscale motions are influenced by molecular architecture, mostly at low shear rates. At high shear rates the observed differences are diminished. The shear rate, at which characteristic times associated with global motion attain the high-shear slope, depends on the topology. The minimum WI systems reach this limit at larger shear rates.

From the above discussion it follows that, in general, the response of the complexes under shear to a large degree follows that of the noncomplexed systems, providing thus the possibility of a more cost-effective experimentation to single (and in principle cheaper) systems, in order to assess the behavior of the corresponding complexes under shear. The findings discussed above can account for the effects that should be expected due to complexation. Furthermore, the described changes in properties associated with the size and

the topology of the HP components may allow a better fine tuning of the physical response of such systems under steady shear conditions.

ACKNOWLEDGMENTS

This work is financially supported by the Hellenic General Secretariat for Research and Technology under the framework of the PENED 2003 program (Grant No. 03EΔ716). S.V.L. acknowledges funding from the Fourth Program of the Division of Chemistry and Materials Science of Russian Academy of Sciences.

[1] T. T. Nguyen and B. I. Shklovskii, J. Chem. Phys. **114**, 5905 (2001).
[2] H. Schiessel, J. Phys.: Condens. Matter **15**, R699 (2003).
[3] D. Leisner and T. Imae, J. Phys. Chem. B **108**, 1798 (2004).
[4] P. K. Maiti and B. Bagchi, Nano Lett. **6**, 2478 (2006).
[5] S. Ulrich, M. Seijo, and S. Stoll, Curr. Opin. Colloid Interface Sci. **11**, 268 (2006).
[6] C. Y. Wang, B. Y. Ren, Z. Tong, F. Zeng, X. X. Liu, S. Z. Wu, and P. Liu, Eur. Polym. J. **41**, 185 (2005).
[7] P. J. Gittins and L. J. Twyman, Supramol. Chem. **15**, 5 (2003).
[8] A. Hult, M. Johansson, and E. Malmstrom, Adv. Polym. Sci. **143**, 1 (1999).
[9] J. M. J. Frechet, Proc. Natl. Acad. Sci. U.S.A. **99**, 4782 (2002).
[10] M. Jonsson and P. Linse, J. Chem. Phys. **115**, 10975 (2001).
[11] A. U. Bielinska, C. L. Chen, J. Johnson, and J. R. Baker, Bioconjugate Chem. **10**, 843 (1999).
[12] J. D. Eichman, A. U. Bielinska, J. F. Kukowska-Latallo, and J. R. Baker, Pharm. Sci. Technol. Today **3**, 232 (2000).
[13] C. L. Gebhart and A. V. Kabanov, J. Controlled Release **73**, 401 (2001).
[14] J. F. Kukowska-Latallo, A. U. Bielinska, J. Johnson, R. Spindlerdagger, D. A. Tomalia, and J. R. Baker, Proc. Natl. Acad. Sci. U.S.A. **93**, 4897 (1996).
[15] D. S. Shah, T. Sakthivel, I. Toth, A. T. Florence, and A. F. Wilderspin, Int. J. Pharm. **208**, 41 (2000).
[16] K. Bogdanov, *Biology in Physics* (Academic, London, 2000).
[17] S. B. Kharchenko, R. M. Kannan, J. J. Cernohous, and S. Venkataramani, Macromolecules **36**, 399 (2003).
[18] S. Pricl, M. Fermeglia, M. Ferrone, and A. Asquini, Carbon **41**, 2269 (2003).
[19] I. Bodnar, A. S. Silva, R. W. Deitcher, N. E. Weisman, Y. H. Kim, and N. J. Wagner, J. Polym. Sci., Part B: Polym. Phys. **38**, 857 (2000).
[20] J. T. Bosko, B. D. Todd, and R. J. Sadus, J. Chem. Phys. **121**, 12050 (2004).
[21] J. R. Dorgan, D. M. Knauss, H. A. Al-Muallem, T. Z. Huang, and D. Vlassopoulos, Macromolecules **36**, 380 (2003).
[22] T. T. Hsieh, C. Tiu, and G. P. Simon, Polymer **42**, 7635 (2001).
[23] S. Uppuluri, F. A. Morrison, and P. R. Dvornic, Macromolecules **33**, 2551 (2000).
[24] I. Bodnar, A. S. Silva, Y. H. Kim, and N. J. Wagner, J. Polym. Sci., Part B: Polym. Phys. **38**, 874 (2000).
[25] J. T. Bosko, B. D. Todd, and R. J. Sadus, J. Chem. Phys. **123**, 034905 (2005).
[26] A. V. Lyulin, D. B. Adolf, and G. R. Davies, Macromolecules **34**, 3783 (2001).
[27] A. V. Lyulin, G. R. Davies, and D. B. Adolf, Macromolecules **33**, 3294 (2000).
[28] C. M. Nunez, B. S. Chiou, A. L. Andrady, and S. A. Khan, Macromolecules **33**, 1720 (2000).
[29] P. F. Sheridan, D. B. Adolf, A. V. Lyulin, I. Neelov, and G. R. Davies, J. Chem. Phys. **117**, 7802 (2002).
[30] A. T. Lee and A. J. McHugh, Macromol. Theory Simul. **10**, 244 (2001).
[31] R. J. Sadus, Mol. Simul. **33**, 569 (2007).
[32] G. O. Shonaike and S. G. Advani, *Advanced Polymeric Materials* (CRC, Boca Raton, 2003).
[33] J. T. Bosko, B. D. Todd, and R. J. Sadus, J. Chem. Phys. **124**, 044910 (2006).
[34] G. K. Dalakoglou, K. Karatasos, S. V. Lyulin, and A. V. Lyulin, J. Chem. Phys. **127**, 214903 (2007).
[35] S. Lyulin, A. Darinskii, and A. Lyulin, e-Polymers **2007**, no. 097.
[36] S. V. Lyulin, A. A. Darinskii, and A. V. Lyulin, Macromolecules **38**, 3990 (2005).
[37] P. Welch and M. Muthukumar, Macromolecules **33**, 6159 (2000).
[38] S. Lyulin, K. Karatasos, A. Darinskii, S. Larin, and A. Lyulin, Soft Matter **4**, 453 (2008).
[39] D. L. Ermak and J. A. McCammon, J. Chem. Phys. **69**, 1352 (1978).
[40] J. Rotne and S. Prager, J. Chem. Phys. **50**, 4831 (1969).
[41] H. Yamakawa, J. Chem. Phys. **53**, 436 (1970).
[42] S. V. Lyulin, L. J. Evers, P. van der Schoot, A. A. Darinskii, A. V. Lyulin, and M. A. J. Michels, Macromolecules **37**, 3049 (2004).
[43] J. P. Ryckaert and A. Bellemans, Chem. Phys. Lett. **30**, 123 (1975).
[44] D. Holter, A. Burgath, and H. Frey, Acta Polym. **48**, 30 (1997).
[45] T. Mulder, A. V. Lyulin, P. van der Schoot, and M. A. J. Michels, Macromolecules **38**, 996 (2005).
[46] H. Wiener, J. Am. Chem. Soc. **69**, 17 (1947).
[47] A. H. Widmann and G. R. Davies, Comput. Theor. Polym. Sci. **8**, 191 (1998).
[48] X. S. Feng, D. Taton, E. L. Chaikof, and Y. Gnanou, J. Am. Chem. Soc. **127**, 10956 (2005).
[49] K. Karatasos, D. B. Adolf, and G. R. Davies, J. Chem. Phys. **115**, 5310 (2001).
[50] S. V. Lyulin, A. A. Darinskii, A. V. Lyulin, and M. A. J. Michels, Macromolecules **37**, 4676 (2004).
[51] J. T. Bosko, B. D. Todd, and R. J. Sadus, J. Chem. Phys. **121**, 1091 (2004).
[52] R. H. Colby, D. C. Boris, W. E. Krause, and S. Dou, Rheol. Acta **46**, 569 (2007).